High precision extrusion of glass tubes

Christopher A. G. Kalnins[1*], Kyle J. Bachus[1], Andrew Gooley[2] and Heike Ebendorff-Heidepriem[1,3]

[1]Institute for Photonics and Advanced Sensing and School of Physical Sciences, University of Adelaide, North Terrace, Adelaide, Australia, 5005

[2]Trajan Scientific and Medical, 7 Argent Place, Ringwood, Victoria, Australia, 3134

[3]ARC Centre of Excellence for Nanoscale BioPhotonics, University of Adelaide, North Terrace, Adelaide, Australia, 5005

*chris.kalnins@adelaide.edu.au Corresponding Author

Abstract

Precision glass tubes for analytical instrumentation often require tight tolerances in their inner and outer diameter, which makes them cumbersome to fabricate. The extrusion method is a potential method for the fabrication of precision glass tubes, however, the effects of die swell and taper which occur during the extrusion process can distort the final product. This work aims to determine the tolerances that can be achieved for glass tubes fabricated using the extrusion method by comparing the extent of the die swell and tapering on tubes extruded under a variety of extrusion parameters. Lead-silicate glass tubes of 6.5 mm outer diameter and 0.50 mm inner diameter were fabricated with a taper of less than 1 % for the outer diameter and less than 5 % for the inner diameter over 200 mm lengths. This target geometry was achieved using a volume flow rate of 4.7 mm^3/s, a glass viscosity of $10^{7.2}$ Pa.s and a die geometry that accommodated a 12 % offset due to die swell. This result indicates the extrusion method is a viable method for producing glass tubes with tight tolerances for applications in analytical instrumentation.

Keywords

Extrusion; fabrication;

Introduction

Precision glass tubes used in analytical instrumentation such as mass spectrometry have specific geometry requirements with dimensional tolerances on the order of 1 % to achieve maximum performance in separation and detection. For example, in mass spectrometry, ion transfer tubes have desired dimensions on the order of 5-6 mm outer diameter (OD) and 500-600 μm inner diameter (ID), where tight ID tolerance is imperative for performance. Tubes fabricated outside of the tolerances can produce a lower signal-to-noise ratio due to losses in the volume of analyte transferred into the detection unit.

Currently, there are several techniques for the fabrication of glass tubes, including drilling and hot-glass drawing. These fabrication techniques present a significant gap in the dynamic range of dimensions that are attainable, wherein glass tubes on the order of 5 - 6 mm OD and 500 μm ID are not trivial to fabricate, especially at lengths beyond 100 mm. Furthermore, the production of these materials with tight tolerances requires significant post-processing techniques such as fire polishing, and in most cases, these tolerances remain beyond the accepted 1 % from specific analytical applications.

Glass billet extrusion offers a method for the fabrication of glass tubes in dimension regions where the current methods lack ability. Also, glass billet extrusion provides a single-step process from glass billet to the desired glass tube where cumbersome post-processing is not required. Several groups have previously demonstrated the capability of the extrusion process to form complex structures in various glasses[1-7]; the flow behavior of glasses during extrusion has also been investigated[8,9]. The previously reported extruded glass elements with various geometries are typically processed further into optical fibres, where modifying the fibre drawing conditions provides additional dimensional control. However, when the extruded glass element is the final product, such as for the glass tubes considered here, tighter tolerance requirements are necessary. To date, there are no detailed publications on the geometry tolerances achievable using the extrusion method.

During extrusion, several glass flow effects need to be considered to achieve the target geometries. One effect is die swell, where the glass exiting the die channel does not retain the same geometry as the die channel but

will expand following the movement of the glass into free space. This effect has been observed previously, where an approximately 12 % increase in diameter for the extrusion of glass rods was observed, irrespective of viscosity and die geometry[10]. However, there was a possible correlation between extrusion speed and the resulting die swell. Modelling shows that interfacial slip between the glass and the die material was the primary mechanism leading to the die swell observed experimentally[9,11]. This modelling has also been applied to more complex structures containing several holes, again demonstrating the friction between the glass and the die is the primary parameter affecting the final extruded geometry of the glass[12]. Another process affecting the final geometry is tapering, where the weight of the already-extruded product "pulls down" on the softened material after it moves through the die channel, thereby stretching the product. Figure 1 shows a diagram explaining the effects of die swell and tapering.

This paper demonstrates the impact of extrusion processing parameters and die dimensions on the geometry of extruded glass tubes, in particular on the effects of tapering and die swell, which results in a deviation of the tube geometry from the die exit geometry. In addition to tube geometry, the roughness of external and internal surfaces of extruded tubes was investigated in relation to extrusion pressure. The advance in understanding the extrusion process was finally used to select extrusion and die parameters that led to tubes with high precision geometry (6.5 ± 0.1 mm outer diameter and 0.50 ± 0.025 mm inner diameter over 200 mm tube length) and high surface finish as required for analytical applications.

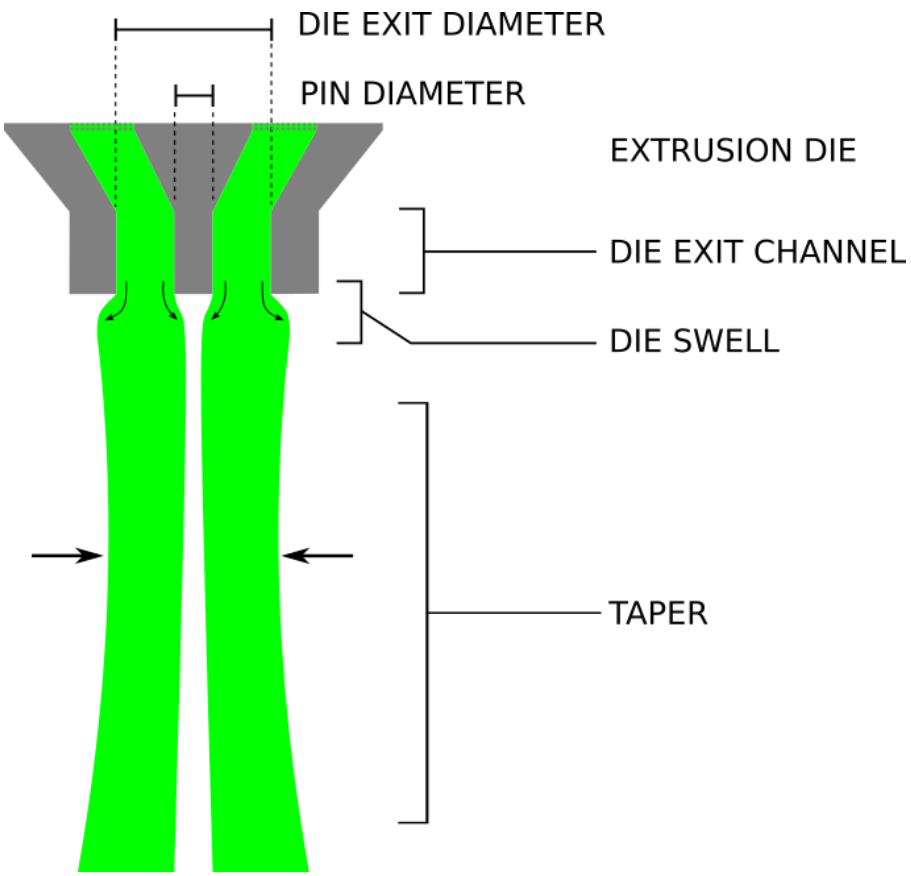

Figure 1: Cross sectional diagram of the extrusion process. Glass (green) is forced down through an extrusion die into the tube geometry; the effects of die swell and tube tapering are also shown.

Method

Glass selection

The commercial lead-silicate glass (F2 from Schott Glass Co.[13]) was selected since this glass has been widely used for extrusion of different structures as well as for investigating extrusion flow behavior using experimental[8] and modelling/simulation[11] approaches. These previous results provided a solid knowledge base for the work presented here.

Extrusion equipment, die design and processing parameters

A customised extrusion machine with a 3-zone customised furnace, was used for all extrusion trials. A more detailed explanation of the process and the precision of the processing parameters controlled by the extrusion machine have been described previously[8], and a schematic is shown in Figure 1.

The glass billets of all extrusion trials had 30 mm diameter and 35 mm length and were polished on all faces. The die design is comprised of a pin suspended in a channel by four struts. This design has been described previously by Belwalker et al.[2]. Extrusion dies were fabricated from stainless steel, which has been proven to be a suitable die material for oxide glasses including F2 due to its high mechanical stability[14]. In addition, and in contrast to other potential die materials such as graphite, stainless steel dies have not shown the propensity for particles transferring from the die material to the extruded glass[14]. Tubes would then require some form of surface treatment to remove embedded particles, whereas it has been shown that the use of metal dies for lead silicate glasses leads to a high-quality surface finish without the need for further surface treatment[15]. Further information on the surface roughness of machined stainless steel extrusion dies has been discussed by Ebendorff-Heidepriem[15].

All the dies used here had the same internal and external structure except the dimensions at the die exit plane. The diameter of the die exit channel (hereafter referred to as exit diameter and which determines the tube outer diameter) and the pin diameter at the exit plane (which determines the tube inner diameter) were varied to investigate the impact of die dimensions on the taper and die swell. The exit and pin diameters of the four die types used were measured using both an optical profiler and a coordinate measuring machine; measurements were performed five times to calculate measurement uncertainties.

For extrusion of oxide glass through metal dies, such as F2 and stainless steel used in this work, a die can only be used once to obtain extruded glass with high optical quality due to the inability to effectively remove the excess glass in the die without damaging the die material. When disassembling the extrusion parts, the metal plate (initially resting on the glass billet) needs to be separated from the excess glass in the die. This separation process typically requires high force and generates a random “break” on the top face of the excess glass in the die. It follows then, that the insertion of a new (squared) glass billet onto the fractured surface creates significant air gaps between recycled and new glass. These air gaps ultimately lead to the presence of bubbles in the extruded glass and significant variation in the quality of each tube, which is unsuitable when high precision is required as for analytical applications. The one-off use of the dies in this work restricted the number

of extrusion trials that could be performed with the available budget. Therefore, it was not possible to do a statistical analysis of results across a large number of trials.

Extrusion speed is defined as the speed of the puncher pushing the 30 mm diameter glass through the extrusion die, not the speed at which the extrudate moves out of the die exit channel. The extrusion temperature is defined as the temperature of the steel body, which houses the die components and glass within the furnace; this body temperature is close to the die temperature and has an uncertainty of ± 1 °C[8]. Extrusion force was used to calculate pressure and is derived from the steady-state regime shown in Figure 2, where the uncertainty in the force is ± 10 % and the uncertainty in the billet cross section is considered negligible in comparison; the uncertainty on pressure values is therefore also ± 10 %.

To compare these extrusion parameters with other glasses and other extrusion systems that might use different billet geometries, the volume flow rate (Q), glass viscosity (η) and extrusion pressure (P) were calculated using measured values for speed (v), temperature (T), force (F) and billet diameter (D).

$$= \frac{}{4} \cdot \quad \cdot \quad ^2 [8] \tag{1}$$

$$_{10}(\ ) = \frac{4065.2}{-137} - 2.314 \ , \ \text{T (°C) and } \eta \text{ (Pa.s) [16]} \tag{2}$$

$$= \frac{}{/4 \cdot \ _2} [8] \tag{3}$$

Extruded tube geometry measurements

During the initial and final stages of the extrusion process, the pressure is not in a steady-state regime; a detailed explanation of this concept has been provided[8]. An example of a pressure profile is shown in Figure 2 where the region of constant pressure indicates the steady-state regime; this region is where the extruded glass yield is obtained. The sections at either end of this extruded glass part, corresponding to non-steady-state conditions, are removed and not used for any analysis presented here.

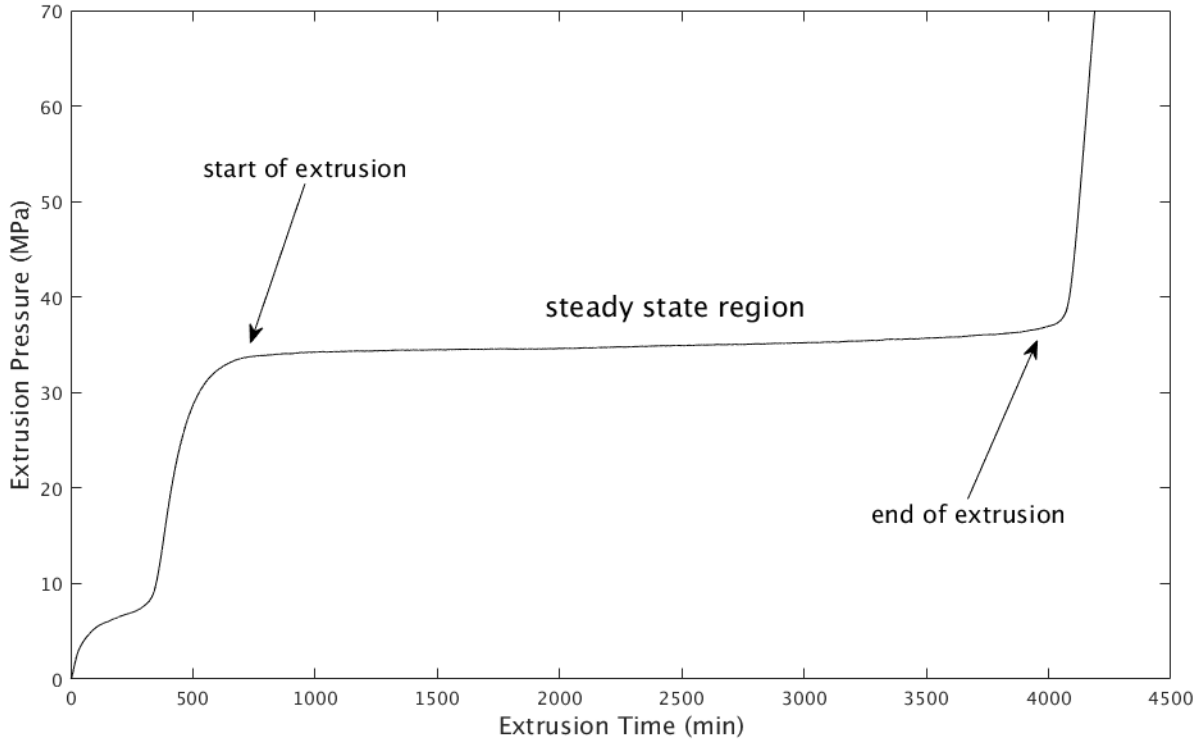

Figure 2: An example of a pressure profile using data from extrusion trial 3. Tube sections are taken from the region where temperature, speed and pressure are consistent.

For the tubes investigated here, the traditional method of cutting glass with a diamond saw introduced roughness and a higher uncertainty during diameter measurements as shown in Figure 3 (right). Therefore, the tubes were precision cleaved by placing them in a jig and rotating them against a ceramic blade to produce a consistent scoring around the circumference before cleaving. This method resulted in clean cross-sections suitable for precision measurements as shown in Figure 3 (left). To measure the geometry of the tubes along their lengths, the extruded tubes of 500 - 600 mm length were cleaved into sections of 200 mm length.

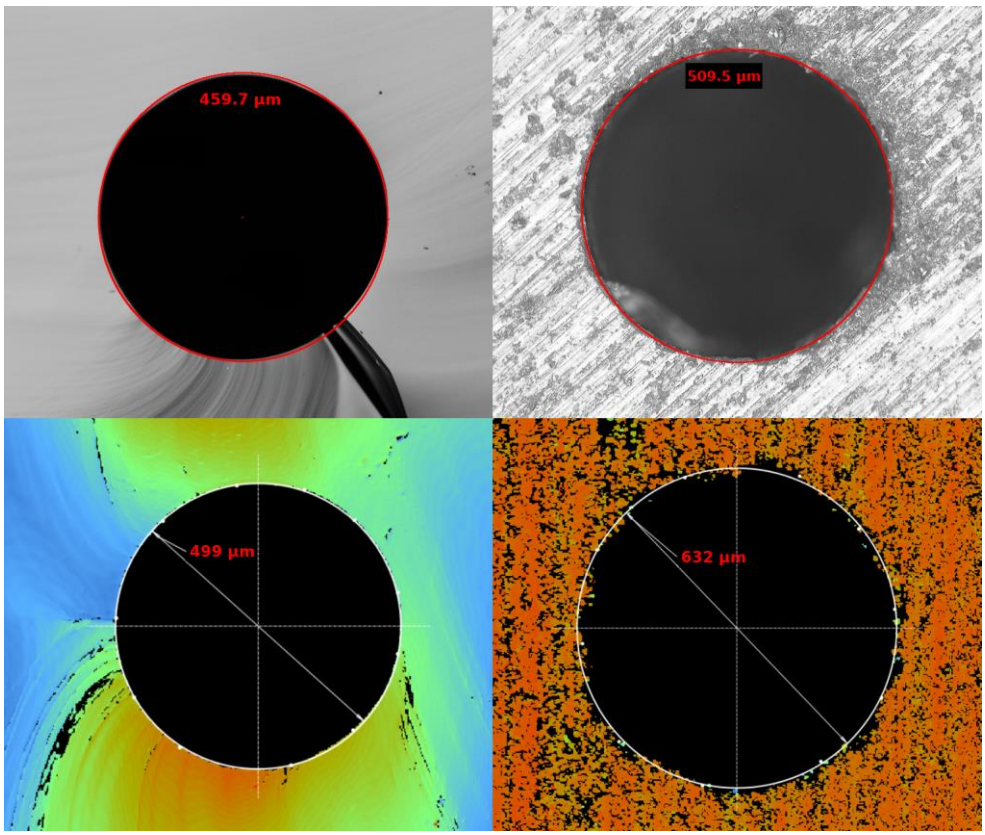

Figure 3: Examples of cross-sectional images from trials 1 and 4 of the inner region of extruded tubes which were cleaved (left column) or sawn (right column). The images were taken with an optical microscope (top row) or an optical profiler (bottom row) and measurement of the inner diameter is indicated by the red circle (top row) or white circle (bottom row).

The tube OD was measured at intervals along the length with calipers (± 0.02 mm), with 0 mm corresponding to the start of extrusion. OD is then plotted against tube length along the steady-state section shown in Figure 2. Slope and uncertainties are then calculated from a linear regression. This slope gives a value for the taper in units of µm/mm. The tube ID was measured by imaging the cross-section of a tube piece with the optical profiler and applying the geometry measurement tools in the software; measurements were repeated five times to determine uncertainties. To quantify the taper, OD is plotted against tube length along the steady-state section shown in Figure 2. Slope and uncertainties are then calculated from a linear regression. This slope gives a value for the taper in µm/mm. In contrast to OD taper, where linear regression of more than ten OD values as a function of tube length was used, the ID taper was calculated using only 2 - 3 ID values measured on both ends of 200 mm lengths cut from an extruded tube. Values for the slope and associated uncertainties

are therefore only calculated using the beginning and end points. Measurement of more points would require cutting the extruded tube into small pieces, which was not possible as tube pieces of 200 mm length were required for further experiments not described in this paper.

Die swell determination

Die swell was quantified using ratios of the corresponding tube and die diameters. For the tube diameters, values at a lateral position with a minimum degree of taper but within the steady-state region were used. As the tube OD is larger than the die exit diameter while the tube ID is smaller than the pin diameter, inverse ratios for tube and die diameters were used - OD/exit and pin/ID. This facilitated the determination of whether die swell for the OD and ID show the same magnitude. Note that the uncertainty for pin/ID ratio was significantly larger (± 0.01) compared with OD/exit ratio (± 0.005) due to the higher relative measurement uncertainties for pin and ID diameter measurements.

Bending

Bending of tubes was measured by aligning one end of the section with a flat surface and measuring how far out from the surface the opposite end of the section extends. This value is then reported as the angle away from parallel for which the tube deviates along the 200 mm length of the section.

Surface quality

The inner surface quality of tubes extruded with a range of different pressures was measured using an optical profiler. Small tube sections were cut and ground to expose the inner surface of the tube as shown in Figure 4. During the grinding process, a high flow of water was used to prevent any waste material from depositing on the surface. Samples were then cleaned ultrasonically before measurement on the optical profiler. Measurements were performed over a 150 x 30 μm area, surface curvature and low frequency undulations were filtered out and the arithmetic average roughness R_a was recorded.

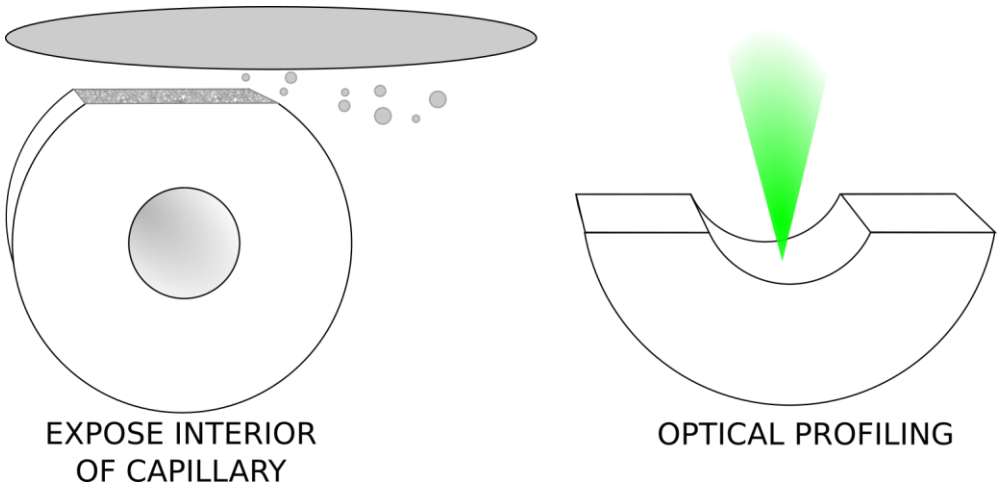

Figure 4: (Left) short sections of tube are cut and the interior surface exposed by grinding the tube. (Right) optical profiling is performed on the exposed inner surface of the tube.

Selection of die types and extrusion parameters

An overview of the die types and extrusion parameters used is shown in Table 1. Based on a range of previous F2 glass extrusion trials of tubes and other structures, the first trial (#1) was performed using die type A at a temperature of 565 °C and a speed of 0.1 mm/min. This trial resulted in a relatively large taper for the extruded tube. Theoretically, taper can be reduced by increasing speed or decreasing temperature. A higher extrusion speed reduces the time the weight of the already extruded glass can exert a tension on the deformable glass close to the hot die exit, thereby reducing taper. A lower temperature enhances glass viscosity, which reduces the extent to which glass can be stretched under a certain tension.

Based on these considerations, the extrusion speed was increased to 0.2 mm/min and die type B with slightly different exit and pin diameters was used in the following extrusion (#2). Following this, the impact of die dimensions for the same speed and temperature was tested. Taking into account the similarity of taper for these two trials irrespective of die dimensions (#2 with die B and #3 with die C), the two different die types (B and C) were also used for the following trials to simultaneously investigate the impact of different die exit and pin diameter on tube die swell. This allowed, with a minimum amount of 6 extrusion trials, the reproducibility of both taper and die swell to be studied.

Building on the results of trials 2 and 3 with 0.2 mm/min speed and 565 ºC temperature, first the impact of reducing the temperature to 560 ºC (#4) and 555 ºC (#5) and then increasing the speed to 0.4 mm/min (#6) was studied. Based on the results of trials 1-6, the following trials (#7 and #8) employed the refined die dimension (die type D) and selected processing conditions (565 ºC, 0.4 mm/min) to achieve the target tube dimensions and target tolerances (OD of 6.5 ± 0.1 mm and ID of 0.5 ± 0.025 mm for at least 200 mm tube length).

Results

Bending

The tubes had minimal measurable bending. Early extrusion trials, such as extrusion 2, had a deviation of approximately 0.3° away from parallel. For later extrusion trials, the extent of bending was too small to obtain a measurable result within measurement uncertainties. These results indicate reproducibly straight extrusions are obtainable with the die types and extrusion parameters used.

Die Swell

With exception to trial 1 with pronounced taper, the die swell for both OD and ID is within measurement uncertainty (Table 2), indicating that die swell is not affected by the taper and die dimensions within the range investigated. For the tube of trial 1 with large taper, the measured ratios OD/exit and pin/die are not only affected by die swell but also taper and therefore are not reliable measures for die swell alone. The consistent die swell values for trials 2 - 8 (1.08 - 1.09 for OD/exit and 1.0 - 1.2 for pin/ID) suggest that for these trials the impact of processing parameters on taper can be investigated irrespective of the die type used. Note that the OD/exit die swell is similar to the experimentally measured values for die swell in various glasses[11]. For the tube ID measurements, the values for pin/ID were found to have more variance, with ratios in the 1.00 - 1.20 region.

To produce tubes with the target OD of 6.50 mm, the extent of die swell was compared prior to fabrication of die type D. Die type C with an exit diameter of 6.50 (used for trials 3 and 5) was found to produce tube OD

values of approximately 7.0 mm, while die type B with an exit diameter of 6.10 mm (used for trials 2, 4 and 6) was found to produce tube OD values of ~6.6 mm (Table 2). Taking these results into account, the exit diameter of die type D (used for trials 7 and 8) was selected to be 6.00 mm. Indeed, this exit diameter adjustment produced tubes with OD of the target dimension of 6.5 ± 0.1mm. The pin of die type D was also guided by extrusions using die types B and C; these dies (used for trials 1-6) were designed to have larger pin diameters of 600 and 650 μm, respectively, to offset the initially estimated die swell effect of approximately 1.1, and resulted in tube IDs of 500-600 μm, indicating these pin diameters are too large to achieve the target tube ID. Therefore, die type D (for trials 7 and 8) was selected to have smaller pin diameter of 550 μm, which was found to produce tubes with ID of the target dimension of 500 ± 25 μm over 200 mm length.

Extrusion Trial	Die Type	Diameter (nominal)		T	ν	log(η)	Q	P
		Exit	Pin					
		(mm)	(μm)	(°C)	(mm/min)	(Pa.s)	(mm^3/s)	(MPa)
1	A	5.90 (6.00)	576 (580)	565	0.1	7.18	1.18	7.4
2	B	6.11 (6.10)	604 (600)	565	0.2	7.18	2.36	13.9
3	C	6.49 (6.50)	653 (650)	565	0.2	7.18	2.36	14.6
4	B	6.10 (6.10)	605 (600)	560	0.2	7.30	2.36	23.2
5	C	6.51 (6.50)	649 (600)	555	0.2	7.41	2.36	28.0
6	B	6.08 (6.10)	608 (600)	565	0.4	7.18	4.71	34.4
7	D	6.00 (6.00)	553 (550)	565	0.4	7.18	4.71	30.7
8	D	5.90 (6.00)	549 (550)	565	0.4	7.18	4.71	30.7
±		0.02	5	1		0.02	0.002	10%

Table 1: Parameters for each extrusion trial: Die and pin diameters with the nominal value given in parenthesis. Extrusion body temperature (T), extrusion speed (ν), glass viscosity (η), volumetric flow rate (Q), and pressure (P). For extrusion 7, the nominal die diameter was used for calculation as the equipment used for measurement was not available. Bottom row indicates absolute uncertainties for values in the column, expect relative uncertainty given for the pressure.

Extrusion Trial	Yield Section	Tube diameter		OD/ID	Taper		OD/die	pin/ID
		OD	ID		OD	ID		
	(mm)	(mm)	(μm)		(μm/mm)	(μm/mm)		
1	270	5.50	460	12.0	2.66*	0.21	0.93	1.25
	520	5.00	407	12.3				
2	140	6.62	542	12.2	0.75	0.09	1.08	1.11
	325	6.47	526	12.3				
3	235	6.97	596	11.7	0.78	0.04	1.07	1.10
	455	6.86	604	11.4				
4	143	6.53	499	13.1	0.44	0.03	1.07	1.21
	325	6.44	504	12.8				
5	119	6.99	591	11.8	0.38	0.01	1.07	1.10
	325	6.91	589	11.7				
6	315	6.56	565	11.6	0.37	0.10	1.08	1.08
	525	6.50	543	12.0				
7	200	6.52	551	11.8	0.39	0.16	1.09	1.00
	400	6.44	519	12.4				
8	105	6.52	496	13.1	0.37	0.03	1.10	1.11
	305	6.44	490	13.1				
±	0.05	0.02	4	0.11	0.05	0.07	0.01	0.01

Table 2: Results of each extrusion trial. Yield Section refers to the position along the length of the extruded tube as measured from the start of extrusion. Bottom row indicates absolute uncertainties for values in the column *The uncertainty of OD Taper for Extrusion 1 is 0.19 μm/mm.

Taper

To explore the relationship between taper for tube OD and ID, the ID values were normalised to OD values. This ID/OD ratio was consistently measured to be 12 ± 1 (Table 2). The extent of the ID taper can, therefore, be inferred from the OD values. The ID taper values are in the range of 0.01 – 0.21 μm/mm, which is not significantly larger than measurement uncertainty, hence no correlation between extrusion parameters and ID taper can be inferred. Due to this, processing parameters are guided only by the OD taper values.

Trial 1, using 565 °C, 0.1 mm/min and die type A, resulted in a tube with pronounced OD taper of 2.66 μm/mm (Table 2). At a speed of 0.1 mm/min, the extrusion time was approximately 310 minutes, during which the extruded section of the tube was hanging into free space. Due to the glass being at elevated temperature as it exits the die exit channel, this softened glass is stretched by the weight of the extruded section. The slow speed of this extrusion provided significant time for this stretching to occur. The large taper changed the OD by 0.43 mm over a 200 mm tube length, which is larger than the target OD tolerance of 0.1 mm.

To overcome this large taper, trials 2 - 6 investigated effects of faster speeds and lower temperatures. The increase of speed from 0.1 mm/min (#1) to 0.2 mm/min (#2, #3) and finally 0.4 mm/min (#6) resulted in a significant reduction in taper from 2.66 to 0.75 - 0.78 and finally 0.37 μm/mm. Likewise for the temperature, as predicted, decrease of the temperature from 565 °C (#2, #3) to 560 °C (#4) and finally 555 °C (#5) led to a reduction in taper from 0.75 - 0.78 to 0.44 and finally 0.38 μm/mm. It is notable that trial 5 with slower speed and lower temperature (0.2 mm/min and 555 °C) and trial 6 with faster speed and higher temperature (0.4 mm/min and 565 °C) lead to the same taper.

As faster speed allows shorter extrusion duration, the following trials 7 and 8 were performed using faster speed and higher temperature (0.4 mm/min and 565 °C) as for trial 6. For these two trials, the dimensions of the die type D were adjusted to precisely counterbalance die swell as described above. Indeed, the extruded tubes of these trials exhibited target OD and ID within the target tolerances.

As described above, all the extrusion trials were conducted using speed and temperature as the set processing parameters, while the pressure was the dependent parameter determined by speed and temperature, whereby the temperature, in turn, affects the glass viscosity. More quantitatively, the extrusion pressure is proportional to speed, viscosity, billet cross section and a so-called die constant[8]. For the small variation in die diameters investigated here, the die constant is approximately equal for all trials. The billet cross section is also the same for all trials, making the pressure only dependent on the set parameters speed and temperature. Therefore, the pressure is a suitable single parameter to explore the impact of extrusion flow on the taper. As the taper decreases with increasing pressure (Tables 1 and 2), the taper was plotted as a function of inverse pressure in Figure 5. This plot reveals reproducibility of taper and pressure for the same speed and temperature. With exception to extrusion 1 with exceptionally large taper, the data can be well fitted with a linear function that yields an intercept close to zero, which is consistent with the prediction that for infinitely high pressure due to infinite speed or infinite glass viscosity (i.e. the extrusion temperature approaching the glass transition point), a taper should be negligible.

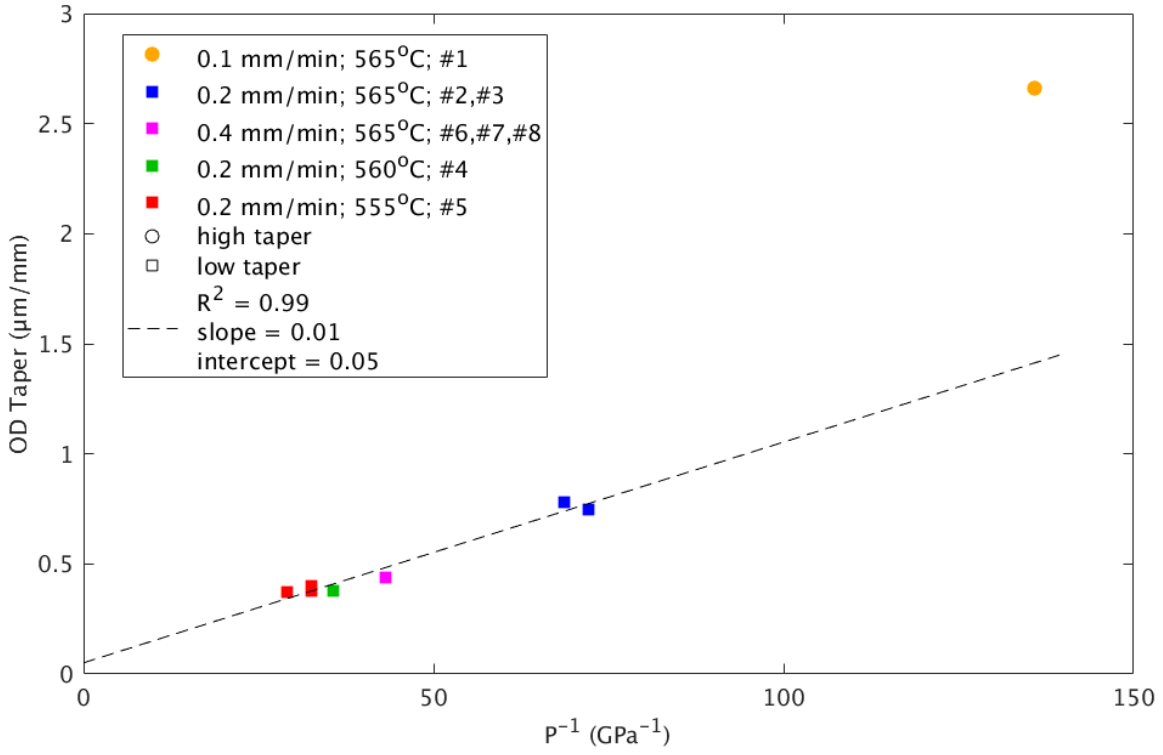

Figure 5: OD taper as a function of inverse extrusion pressure. As extrusion pressure is increased, taper reduces. Linear fit is applied to trials 2 – 8, note how trial 1 has significantly higher taper and does not fit to this trend.

In this study, the target dimension for the tube is to have less than 0.1mm OD variation over 200mm lengths, which equals a taper of 0.5 μm/mm. This target is achieved for trials 4-8, showing a taper less than 0.5 μm/mm. Increasing the tube length within OD tolerance of 0.1mm, e.g. to 1 m length, would decrease taper target to 0.1 μm/mm, requiring a pressure of 110 MPa, which could lead to die damage. This example illustrates that knowledge of taper as a function of pressure allows prediction of the possible yield within tolerances and for maximum possible pressure to avoid die damage. Note that the slope of the linear function of taper versus inverse pressure is expected to depend on the length of the hot zone below the die exit, where the glass is sufficiently soft to be able to be stretched under tension. The hot zone length depends on the furnace and setup used.

Surface Quality

Results for surface roughness measurements are shown in Table 3, and the corresponding surface profiles are presented in Figure 6.

Theoretically, for extrusions performed at a sufficiently high temperature, the viscosity of the glass may be low enough for surface tension effects to help smooth any rough features on the surface as it moves out of the die exit channel[15]. However, as the temperature is decreased, hence increasing extrusion pressure, this fire polishing effect will not be as effective.

Extrusion trial	Speed (mm/min)	Temperature (°C)	Pressure (MPa)	R_a inner (nm)
#1	0.1	565	7.4	8 ± 0.4
#3	0.2	565	14.6	58 ± 0.2
#4	0.2	560	23.2	30 ± 2.6
#8	0.4	565	30.7	16 ± 1.5

Table 3: Arithmetic average roughness (R_a) measurements performed on the interior of tubes extruded with different pressure values.

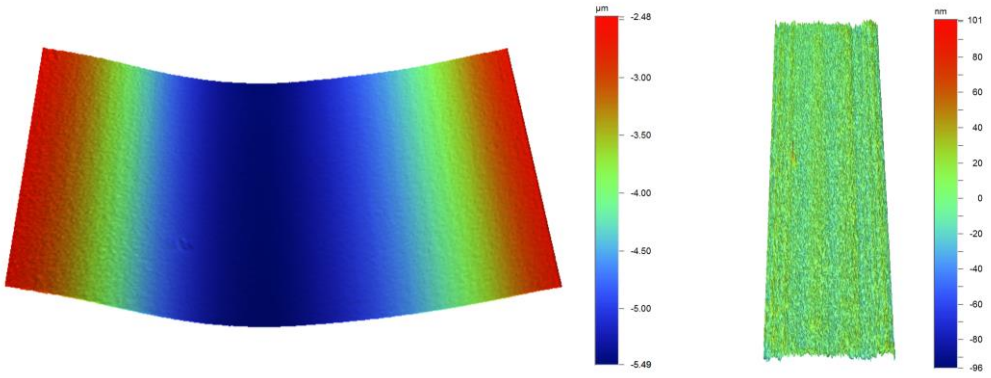

Figure 6: Inner surface of trial 1 as measured using the optical profiler, (left) raw data and (right) following masking and filtering.

The initial trials 1 - 3 therefore used extrusion parameters resulting in low pressure, approximately 7 - 14 MPa. However, as described above, higher speed or lower temperatures, and hence higher pressures were eventually necessary to reduce tapering below the target for trials 4-8. The use of higher pressure necessitated further investigation into the impact of pressure on surface roughness to determine if a compromise would need to be made between the tube taper and the surface roughness.

For inner surfaces, low roughness was measured for trial 1, which had a low extrusion pressure. However, trials 3, 4 and 8 showed no correlation between pressure and roughness. The roughness of outer surfaces was consistently in the range of R_a = 5 – 15 nm, with little correlation to extrusion pressure. This relationship (or lack thereof) suggests other factors such as the roughness of the extrusion die exit and pin are the critical parameters that might affect the surface roughness. Note that the surface finish of the die exit channel surfaces can be improved using polishing, which has been demonstrated previously using 3D printed titanium extrusion dies[15].

Summary and conclusions

The taper decreases with increasing speed and decreasing temperature; for higher speed, the glass is hanging under its weight for a shorter time, and at lower temperature, the glass is in a more viscous state during the period it is hanging. Increase in speed or decrease in temperature is accompanied by increaseing pressure. However, this did not produce any significant increase in surface roughness of the extruded tubes.

More quantitatively, the taper decreases linearly with the inverse of the pressure for OD tapers < 1 μm/mm. This dependence of the taper on extrusion parameters shows that either the option of slower speed and lower temperature (0.2 mm/min and 555 °C) or the option of faster speed and higher temperature (0.4 mm/min and

565 ºC) yield the same taper. Of these two options, faster speed is preferred as it enables the production of tubes in a shorter time. Corresponding volume flow rate and glass viscosity are 2.4 mm^3/s and $10^{7.4}$ Pa.s for the slower speed option and 4.7 mm^3/s and $10^{7.2}$ Pa.s for the faster speed option.

Excluding preliminary trial 1 with large taper, die swell is independent of die geometry, speed and temperature within the parameter range studied. Therefore, die exit and pin diameters were the main parameters affecting the final inner and outer diameters of the extruded tubes with minimal taper. The magnitude of die swell was calculated and die geometries adjusted accordingly. A die exit diameter of 6.00 mm and a pin diameter of 550 μm was found to produce tubes with an OD of 6.50 mm and an ID of 500 μm.

Glass tubes with target geometry of OD = 6.50 ± 0.1 mm and ID = 500 ± 25 μm over 200 mm length (i.e. with target tapers of 0.50 μm/mm for OD and 0.125 μm/mm) were fabricated using extrusion die dimensions that compensated for die swell and extrusion processing conditions that minimised tapering of the extruded product. More precisely, tubes with OD taper of 0.38 μm/mm (i.e. 1%) and ID taper of 0.10 μm/mm (i.e. 4%). This work demonstrates that the extrusion process can be utilised to obtain structures within the tolerances for specific analytical applications.

Acknowledgments

Financial support is acknowledged from the Australian Research Council under grant LP160100657 and through the Research Hub for Australian Copper-Uranium, also from the South Australian Government and Trajan Scientific and Medical under the South Australian Photonics Catalyst Program. This work was performed at the Optofab node of the Australian National Fabrication Facility under the National Collaborative Research Infrastructure Strategy utilising Commonwealth and South Australia State Government funding.

References

[1] Ebendorff-Heidepriem H, Monro TM. Extrusion of complex preforms for microstructured optical fibers. Opt Express, 2007;15:15086–15092.

[2] Belwalkar A, Xiao H, Misiolek WZ, et al. Extruded tellurite glass optical fiber preforms. J Mater Process Technol, 2010;210:2016–2022.

[3] Bei J, Monro TM, Hemming A, et al. Fabrication of extruded fluoroindate optical fibers. Opt Mater Express, 2013;3:318–328.

[4] Zhu M, Wang X, Pan Z, et al. Fabrication of an IR hollow-core bragg fiber based on chalcogenide glass extrusion. Appl Phys A Mater Sci Process, 2015;119:455-460.

[5] Gattass RR, Rhonehouse D, Gibson D, et al. Infrared glass-based negative-curvature anti-resonant fibers fabricated through extrusion. Opt Express, 2016;24:25697-25703.

[6] Tao G, Shabahang S, Banaei E-H, et al. Multimaterial preform coextrusion for robust chalcogenide optical fibers and tapers. Opt Lett, 2012;37:2751-2753.

[7] Tao G, Shabahang S, Ren H, et al. Robust multimaterial tellurium-based chalcogenide glass fibers for mid-wave and long-wave infrared transmission. Opt Lett, 2014;39:4009-4012.

[8] Ebendorff-Heidepriem H, Monro TM. Analysis of glass flow during extrusion of optical fiber preforms. Opti Mater Express, 2012;2:304–320.

[9] Zhang ZF, Zhang Y. Finite element simulation of extrusion of optical fiber preforms: Effects of wall slip. Opt Fiber Technol, 2016;28:18–22.

[10] Mayer HJ, Stiehl C, Roeder E. Applying the finite-element method to determine the die swell phenomenon during the extrusion of glass rods with non- circular cross-sections. J Mater Process Technol, 1997;70:145–150.

[11] Trabelssi M, Ebendorff-Heidepriem H, Richardson KC, et al. Computational modeling of die swell of extruded glass preforms at high viscosity. J Am Cer Soc, 2014;97:1572–1581.

[12] Trabelssi M, Ebendorff-Heidepriem H, Richardson KC, et al. Computational Modeling of Hole Distortion in Extruded Microstructured Optical Fiber Glass Preforms. J Lightwave Technol, 2015;33:424–431.

[13] Schott Glass Company
www.schott.com/advanced_optics/english/index.html
(accessed 2nd May 2018)

[14] Bei J, Monro T, Hemming A, et al. Reduction of scattering losses in fluoroindate glass fibers. Opt Mater Express, 2013;3:1285–1301.

[15] Ebendorff-Heidepriem H, Schuppich J, Dowler A, et al. 3D-printed extrusion dies: a versatile approach to optical material processing. Opt Mater Express, 2014;4:1494-1504.

[16] Chen, M. J, Stokes, Y. M., et al. Drawing tubular fibres: experiments versus mathematical modelling. Opt Mater Express, 2016;6:166-180

[17] Tronnolone H, Stokes YM, Foo HTC, et al. Gravitational extension of a fluid cylinder with internal structure. J Fluid Mech, 2016;790:308–338.